1-72-431
PREPRINT

NASA TM X- 66108

VARIATIONS IN THE STRATOSPHERIC OZONE FIELD INFERRED FROM NIMBUS SATELLITE OBSERVATIONS

(NASA-TM-X-66108) VARIATIONS IN THE STRATOSPHERIC OZONE FIELD INFERRED FROM NIMBUS SATELLITE OBSERVATIONS A.J. Krueger, et al (NASA) Oct. 1972 18 p CSCL 04A G3/13 N73-12397 Unclas 49150

ARLIN J. KRUEGER
DONALD F. HEATH
CARLTON L. MATEER

OCTOBER 1972

GSFC
GODDARD SPACE FLIGHT CENTER
GREENBELT, MARYLAND

Reproduced by
NATIONAL TECHNICAL
INFORMATION SERVICE
U S Department of Commerce
Springfield VA 22151

X-651-72-431
Preprint

VARIATIONS IN THE STRATOSPHERIC OZONE FIELD INFERRED FROM NIMBUS SATELLITE OBSERVATIONS

Arlin J. Krueger
Donald F. Heath
Carlton L. Mateer

October 1972

GODDARD SPACE FLIGHT CENTER
Greenbelt, Maryland

PRECEDING PAGE BLANK NOT FILMED

VARIATIONS IN THE STRATOSPHERIC OZONE FIELD INFERRED FROM NIMBUS SATELLITE OBSERVATIONS

Arlin J. Krueger and Donald F. Heath
Goddard Space Flight Center
Greenbelt, Maryland

and

Carlton L. Mateer
Atmospheric Environment Service
4905 Dufferin Street
Downsview, Ontario

ABSTRACT

The ultraviolet earth radiance data from the Backscatter Ultraviolet Experiment on Nimbus 4 have been inverted to infer ozone profiles using a single Rayleigh scattering model. Two methods of solution give essentially the same results. Comparisons of these profiles with simultaneous rocket sounding data shows satisfactory agreement at low and middle latitudes.

Vertical cross sections of ozone mixing ratio along the orbital tracks indicate that while the gross characteristics of the ozone field above 10 mb are under photochemical control, the influence of atmospheric motions can be found up to the 4 mb level.

Preceding page blank

PRECEDING PAGE BLANK NOT FILMED

CONTENTS

Preceding page blank

ILLUSTRATIONS

VARIATIONS IN THE STRATOSPHERIC OZONE FIELD INFERRED FROM NIMBUS SATELLITE OBSERVATIONS

I. INTRODUCTION

This paper deals with the high level ozone distribution as inferred from measurements of backscattered ultraviolet (BUV) earth radiances from Nimbus 4 satellite at 7 discrete wavelengths between 2555 and 3058 Å. The instrument is described by Heath, et al (1973). We will briefly discuss the relevant physical processes and the mathematical inversion techniques, and will present some comparisons with rocket soundings and some sample BUV results.

The possibility of estimating the ozone profile from backscattered ultraviolet measurements was suggested by Singer and Wentworth (1957). Satellite applications on the technique have been reported by Rawcliffe and Elliott (1966), Krasnopol'skiy (1966), Iozenas et al (1968), Iozenas et al (1969a, 1969b), and Anderson et al (1969). The present experiment uses a "dedicated" instrument, that is to say one designed specifically for the inference of ozone from the earth radiance. The selection of the wavelengths to be sampled was based on the potential information content of the observations and special attention was paid to the problem of reducing stray light within the instrument and to substantially reducing the sensitivity of the instrument to changes in the polarization of the backscattered radiance.

II. PHYSICAL PRINCIPLES

The physical basis of the technique is illustrated in Figure 1, which shows the relative amount of energy backscattered at various levels in the atmosphere for several of the BUV wavelengths. In general, the backscattered radiance comes from a fairly well-defined effective scattering layer. For a given ozone distribution, viewing geometry, and solar zenith angle, the position of the layer in the vertical depends primarily on the ozone absorption coefficient and, hence, by varying the wavelength of observation (and thereby the absorption coefficient), we obtain the vertical scanning effect illustrated in Figure 1. For those wavelengths which do not penetrate through the main ozone layer (2975Å and shorter wavelengths in the case shown) to the dense troposphere, a physical model which involves only single scattering is quite adequate. In the present paper, we restrict our discussion to this simple single-scattering case and, consequently, to the inference of the vertical ozone

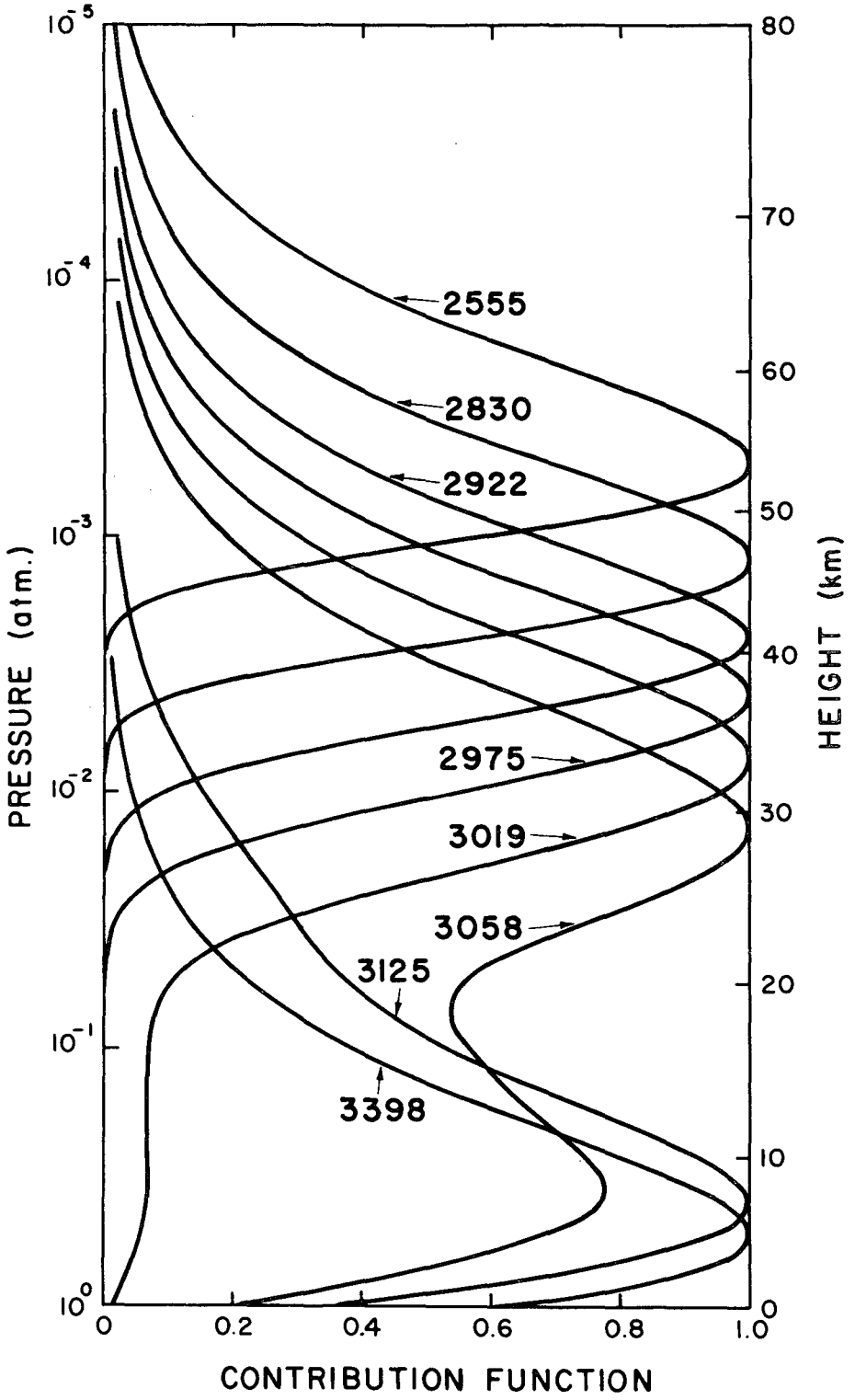

Figure 1. Contribution to satellite-observed nadir-direction backscattered radiance from various levels in the atmosphere. Curves are normalized to unity at level of maximum contribution. All orders of molecular scattering are included. Solar zenith angle = 60°. Total ozone = 336 m atm-cm.

distribution between about 30 and 50 km (10 and 1 mb). Methods of estimating the vertical distribution below 30 km have been discussed by Herman and Yarger (1969) and Yarger (1970). We recognize, of course, that the presence of aerosols above 30 km would serve primarily to increase the backscattered radiance and would lead to the inference of ozone densities that would be too low.

III. INVERSION SOLUTIONS

The ozone distributions presented in this paper have been inferred by two different methods. The basic elements of each of these methods are described below:

Method A: This method utilizes a linearization based on first order partial derivatives (Dütsch, 1959) to set up the basic equations to be solved. The solution is then obtained by the iterative procedure described by Smith (1970). The method starts with a first-guess ozone profile based on Green's (1964) three-parameter profile which gives a simple exponential distribution at high levels (see also Rawcliffe and Elliott, 1966). The selection of those wavelengths which would not be "contaminated" by multiple scattering was based on a prior study considering total ozone and solar zenith angle. The method is rather slow computationally because of the need to recompute the first order partial derivatives for each new iteration. In addition, because of the use of a single exponential slope at high levels, the first guess is frequently poor near 30 km and many iterations are necessary to correct this. In practice, a maximum of 15 iterations has been permitted in routine evaluations. Properties of this method have been discussed by Mateer (1972).

Method B: The basic equations to be solved are set up according to the Pressure Increment (PI) method described by Yarger (1970). The solution of these equations is obtained as an eigenvector expansion (Mateer, 1965), wherein the first three eigenvector contributions appear in the final solution with full amplitude and the fourth and subsequent eigenvector contributions appear with a reduced amplitude to minimize the amplification of random measurement noise in the solution. This may be considered as a modified Twomey (1963) method and the mathematical questions involved have been discussed thoroughly by Strand (1972). The equations appear to be very nearly linear in practice and no iterations are performed. Method B includes corrections for variations in the earth-sun radius vector and wavelengths which penetrate the ozone layer, and which would therefore be contaminated by multiple scattering,

are rejected internally in the program. Finally, the first-guess ozone profile is obtained by using the four shortest wavelengths to compute a high-level exponential ozone profile, which is then joined to a three-parameter Green (1964) profile in which total ozone is conserved. In effect, this gives a two-slope profile above 30 km as the first-guess and avoids the problems experienced in Method A. The solution computing time is about one-fifth of that for Method A.

Through most of the 30-50 km region, these two methods give essentially the same results, within about 10-15 percent. However, near 30 km, differences may be larger because of a different number of wavelengths used in the two methods or because of large differences in the first guess.

IV. COMPARISONS WITH ROCKET SOUNDINGS

The validity of the inversion results depends significantly on the correctness of the physical model assumptions and on instrumental factors such as calibration accuracy and residual polarization sensitivity. Therefore, the BUV flight program has included independent direct ozone soundings throughout the life of the experiment. Rockets are required because the BUV inversion results apply principally above balloon flight levels. Two types of rocket instruments have been utilized. An optical ozonesonde, which was used for evaluation of OGO 4 satellite ozone data (Krueger, 1969), was flown on Arcas rockets for 12 comparisons with the BUV between June 1970 and May 1972. The launch sites, at six latitudes from 9°N to 64°N, were selected to evaluate BUV profiles over a large range of solar zenith angles and geographic conditions. The second type of instrument, a chemiluminescent ozonesonde (Hilsenrath, et al, 1969) was flown at Point Barrow, Alaska in May 1972 to test inversion results in the limiting case of the sun very close to the horizon.

Although the results are available only for the earlier comparisons, the first cases demonstrate that essentially the same ozone density distributions are found by the BUV and rockets at low and middle latitudes. Figure 2 illustrates the ozone partial pressure distributions found at Point Mugu, Calif. (34°N, 119°W) on June 18, 1970. The independent variable is air pressure in millibars; a height scale in kilometers is given on the right-hand border for reference. Above 10 mb the slope and absolute magnitude of the BUV profile (shown by the thin line) agree well with the rocket results (thick line) up to the 1 mb level. Below 10 mb, the agreement continues to be satisfactory to the level of maximum ozone density if the 2975Å wavelength is excluded from the inversion (see curve labeled w/o λ2975). The ozone optical depth at this wavelength is insufficient to prevent multiply scattered light from influencing

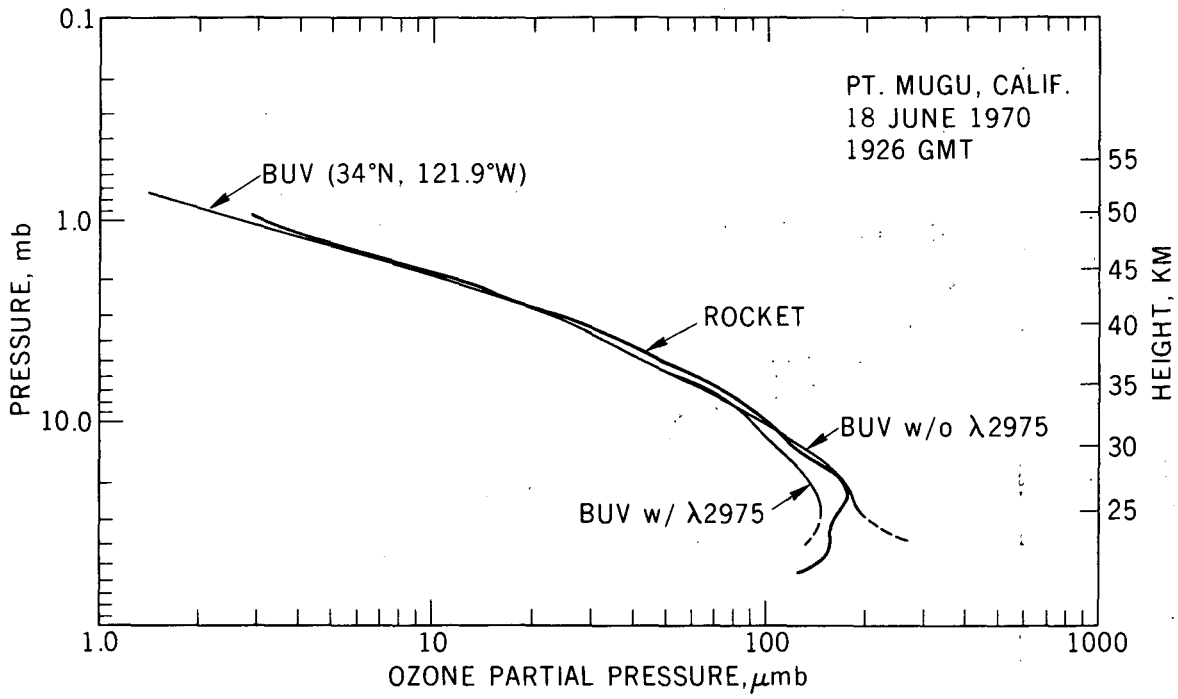

Figure 2. Ozone distributions determined simultaneously with the BUV and the ROCOZ optical rocketsonde at Point Mugu, California on June 18, 1970.

the earth radiance under the conditions of the comparison (solar zenith angle = 12°, total ozone = .331 atm cm). The effect of this additional contribution to the radiance is to cause the inversion to underestimate the ozone below 10 mb as shown by the curve labeled BUV w/λ2975. It is clear from this, that with judicious use of the BUV wavelengths, the single scattering model is not seriously in error and the instrument calibration is in reasonable agreement with the rocket parameters.

The ozone density, with a dynamic range of nearly 100 in the stratosphere, has a limited usefulness in portrayal of global ozone fields. The ozone-to-air mass mixing ratio is a more convenient parameter in that the scale is compressed. This quantity is also a conservative property at levels where the ozone lifetime is long. The results from the Point Mugu comparison in terms of mixing ratio in μgm/gm vs air pressure in mb are given in Figure 3. The rocket data, evaluated at one km intervals from 21 to 50 km, are shown by the solid line and the probable errors are indicated by the bars at each level. The air pressure at each height is derived from an independent rocket sounding of air temperature. The BUV results, shown with a dashed line, are within 20% of the rocket data. The regions of disagreement are near 10 mb and above 1 mb.

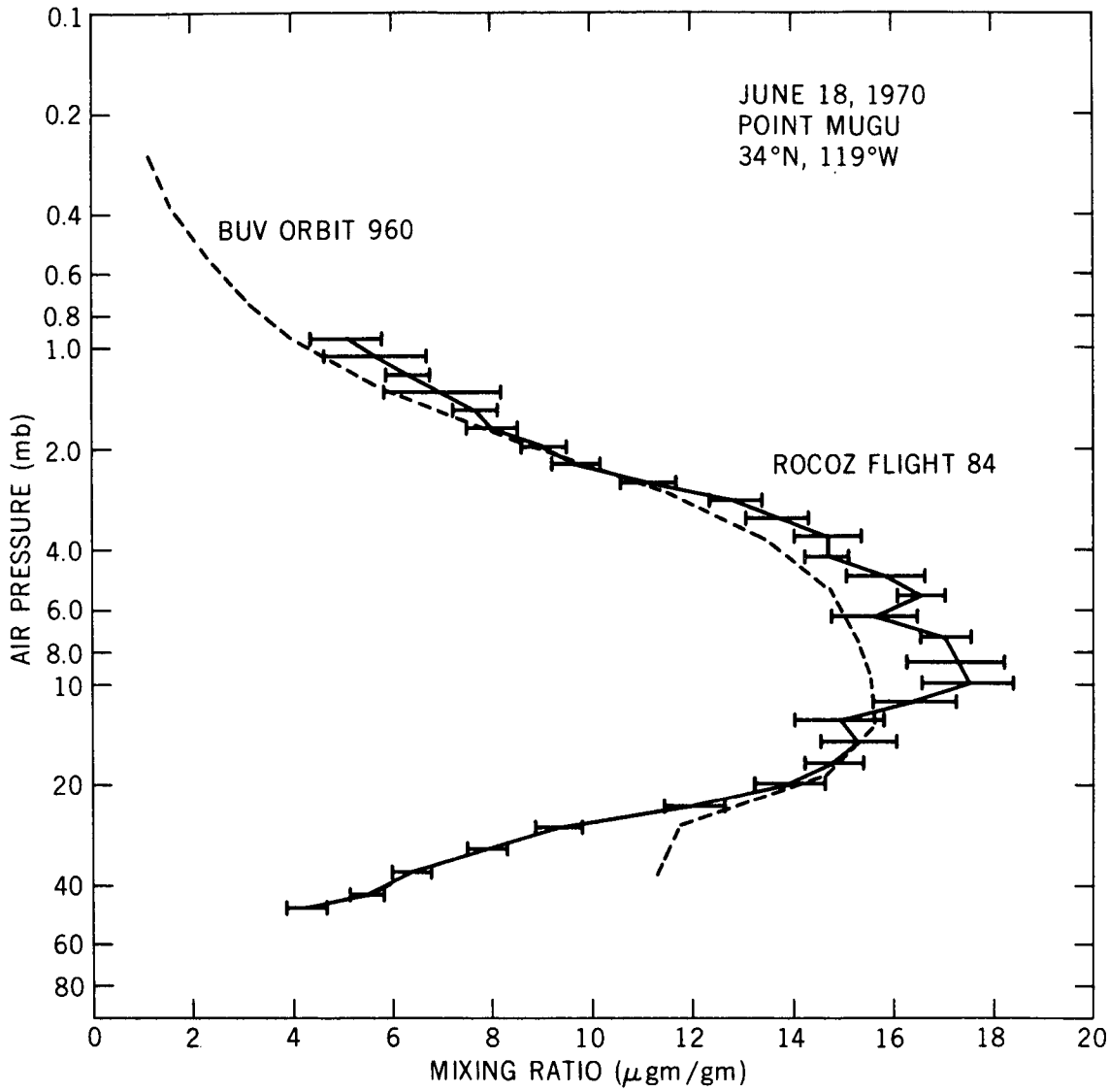

Figure 3. Comparison of the ozone mass mixing ratio distributions derived from the BUV and ROCOZ data on June 18, 1970 at Point Mugu, California.

A second comparison, at a lower latitude and with a different mixing ratio distribution, is shown in Figure 4. The rocket was launched at Barking Sands, Hawaii (22°N, 158°W) on February 24, 1971. The results are again shown at 1 km intervals from 21 to 50 km. In this case, the rocket probable errors are large above 1.2 mb (47 km). As in the Point Mugu comparison, the BUV inversion results have the same character as the rocket distribution. The small scale features in the rocket data would not be expected to be reproduced in the satellite profile because of the filtering properties of the technique.

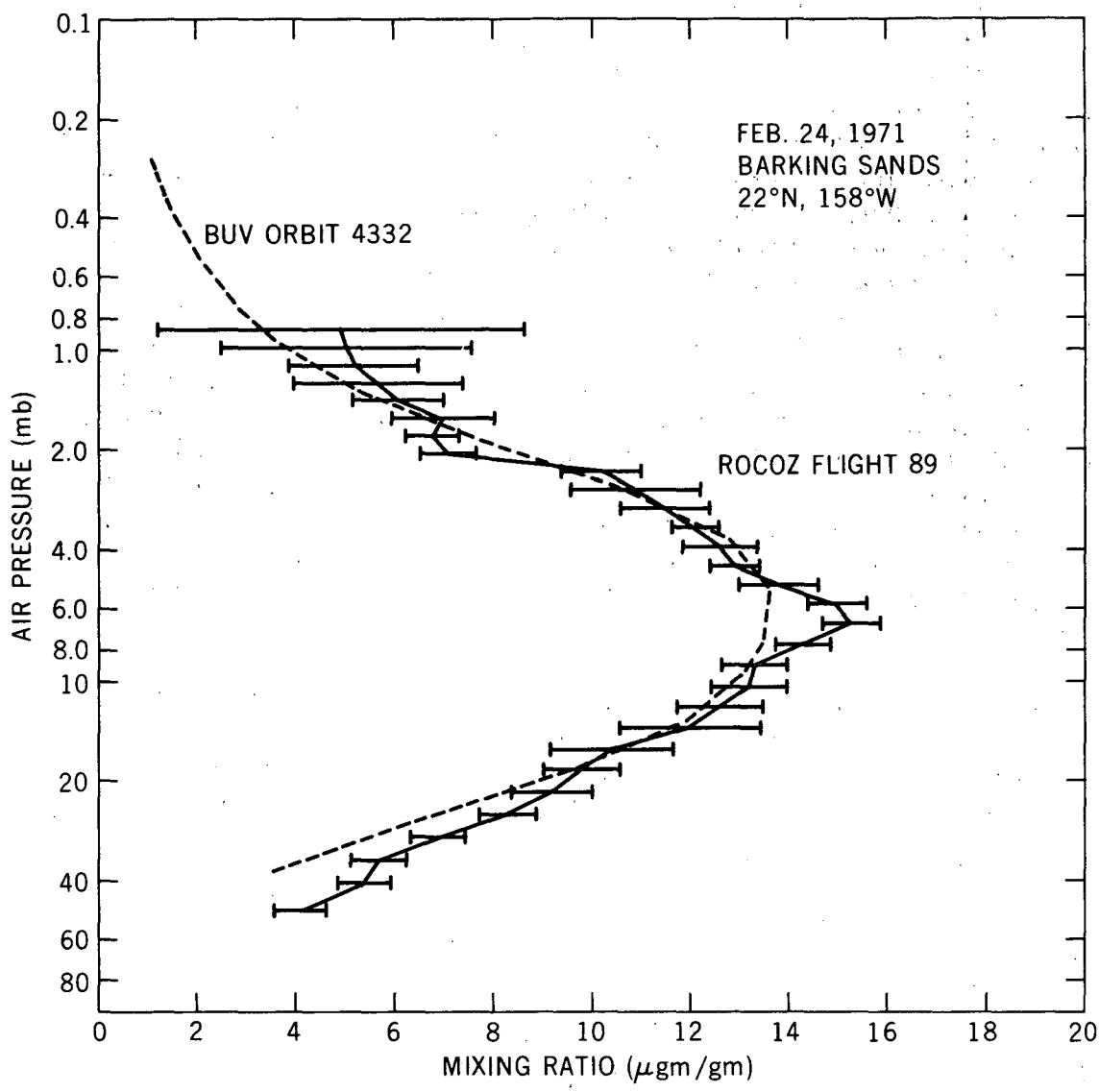

Figure 4. Comparison of the ozone mass mixing ratio distributions from the BUV and ROCOZ instruments on February 24, 1971 at Barking Sands, Hawaii.

In both comparisons, there is a tendency for BUV inversions to underestimate near the 1 and 10 mb levels. In another comparison at 55°N the difference at 10 mb was found to be larger. It is not clear to what extent these discrepancies may be attributed to deficiencies in the physical model, especially the contributions of stratospheric aerosols to the backscattered radiances, or to possible errors in the rocket sounding technique. Until the problem is completely assessed, the results and inferences in the following sections should be treated as preliminary.

V. RESULTS FROM REPRESENTATIVE ORBITS

The polar orbit of Nimbus 4 enables measurements to be made along a track from the southern to the northern terminators, timed near local noon. Because of the orbital inclination, the latitudes observed are between 80°S and 80°N. Approximately 100 ozone profiles can be derived on each orbit. These profiles tend to change rather slowly with latitude, thus leading one to believe that the smallest scale structure in high level ozone is larger than the 195 km distance between soundings. With this apparent continuity, one can construct mixing ratio cross sections along the orbital track with little smoothing. Figure 5 illustrates these pseudo-meridional cross sections for four individual orbits in each of the seasons. The two charts on the left show representative orbits close in time to the vernal (top) and autumnal (bottom) equinoxes and, on the right, northern summer (top) and northern winter (bottom). Although the model for the inversion predicts accurate profiles between 10 and 1 mb, the rocket comparisons suggest that the profiles may contain useful information down to the level of maximum ozone density. For this reason, mixing ratio isolines are shown between 40 and 0.6 mb, extending from the terminator to 80° at the sunlit pole.

Two dominant spatial and temporal characteristics have been found in these cross sections: 1) highly persistent, global-scale features which change only slightly from orbit-to-orbit but vary with season and 2) small-scale transient modulations on the global contours with sizes of 2° to 10° along the orbital track.

The persistent features are characterized by a tropical maximum centered near 10 mb with an extension of this maximum to higher altitudes in the winter hemisphere. Above these regions of high mixing ratio, the contours have little structure. In the summer hemisphere, the horizontal and vertical gradients are weak. The tropical maximum tends to be outlined by the 14 μgm/gm contour. The latitude of the apparent center shifts with the solar declination into the summer hemisphere as can be found in the right-hand diagrams. The shifts appear to be about half the declination angle. In the left-hand diagrams, which represent equinoxial conditions, the tropical maxima are centered over the equator.

The extension into the winter hemisphere is roughly outlined by the 12 μgm/gm contour. The average boundaries of this feature are quite persistent; however, the development at the onset of winter seems to be much less systematic than the regular seasonal shifts of the tropical maximum. Isolated maxima are quite generally found near the terminus of these extensions although hemispheric differences in position and amplitude appear to exist. In the

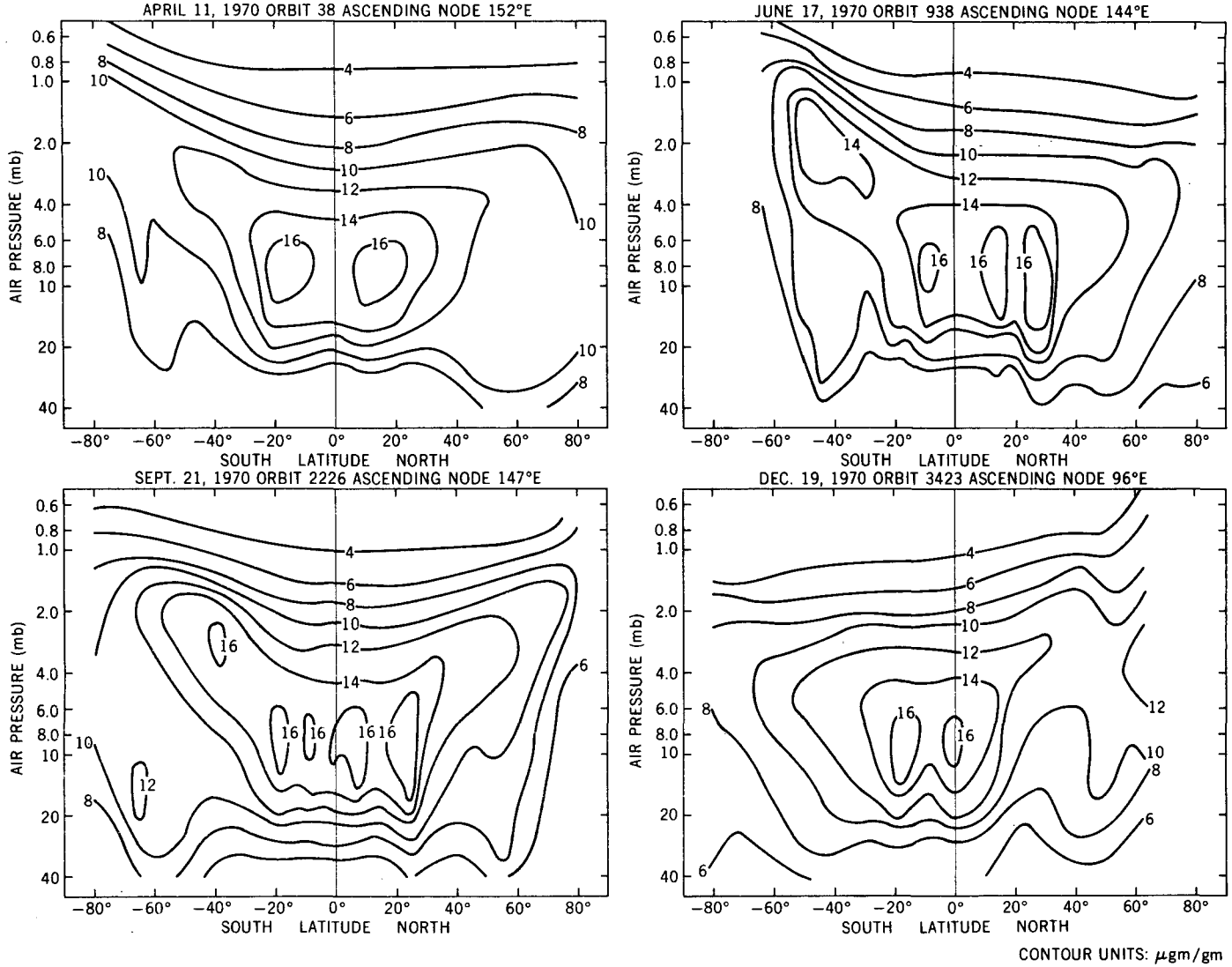

Figure 5. Pseudo-meridional cross sections of ozone mass mixing ratio derived from BUV data during four orbits of Nimbus 4. The cross sections are selected to illustrate seasonal changes in the gross characteristics of the high level ozone distribution and transient, small-scale features found in individual orbits. The northern hemisphere seasons corresponding to these cross sections are spring (upper left), summer (upper right), fall (lower left), and winter (lower right).

southern hemisphere winter the maximum is found centered near 40-45°S at the 2-3 mb levels. At the December solstice, however, the maximum seems to be in the polar night north of 60° latitude, at the 4 mb level. Data from February, 1971 show somewhat greater similarities with the southern hemisphere winter contours.

At the highest altitudes in these cross sections, the smooth contours are due, in part, to a loss of sensitivity above 1 mb. However, these contours show regular changes with latitude and season which appear to be inversely related to the amount of insolation. The lowest values are found at the summer pole and, at the equinoxes, near the equator. The highest values occur in the winter polar regions.

The second class of dominant characteristics, the small-scale transient modulations on the general pattern, usually appear only below the 4 mb level. These can be found in Figure 5 as cells of 16 μgm/gm embedded in the tropical maximum and, at higher latitudes, as tongues of higher mixing ratio air extending below the 10 mb level or lower mixing ratio air extending above that level. The low latitude cells are not correlated between orbits, indicating a zonal size scale on the same order as the meridional size which is normally less than 10°. An estimate of the life time has not been possible, although if the cells are geographically fixed, an upper limit of one week can be set from the Nimbus 4 orbital retrace period. Because of the size of these features associations with tropospheric cloud systems have been examined. Such a correspondence could be interpreted either as a coupled dynamic effect or as a potential artifact in the measurement technique. Pictures from the Image Dissector Camera System (Nimbus Project, 1970) on the same spacecraft show no apparent relationship at any latitude.

VI. CONCLUSIONS

The preliminary results from the Backscatter Ultraviolet Experiment on Nimbus 4 show characteristics with a wide spectrum of temporal and spatial scales during the first year of operation. The ozone field at levels above 10 mb is dominated by persistent contours of global scale which shift slowly with season. Below about 4 mb these contours are modulated by transient changes with sizes generally less than 10° of latitude.

It is believed that the global scale features represent the tendency for establishment of photochemical equilibrium above 10 mb. Because of the direct influence of transport by the general circulation, the contours are not likely to represent a static equilibrium ozone field. Other indirect effects of

temperature changes associated with the air motions also affect the equilibrium mixing ratio through the temperature coefficients of the chemical reactions. A complete analysis will require a satisfactory photochemical model and the stratospheric temperature distribution, perhaps as observed with the Selective Chopper Radiometer (Barnett et al, 1972), also on Nimbus 4. The small scale, transient features would require vertical motion elements or a non-uniform spatial distribution of other chemically-active constituents for an explanation. At the higher latitudes, the downward projecting tongues of enhanced mixing ratio seem to be associated with locally warmer areas found in data from the highest altitude channel of the Satellite Infrared Spectrometer Experiment (Nimbus Project, 1970). Such an association, if borne out in further analysis, would be clear evidence for subsidence.

The high level ozone distributions thus seem to contain new information about the photochemistry of ozone and air motions in the stratosphere. Data acquired in the more than two years of operation may also provide a base line for evaluation of natural long term changes due to the solar cycle and possible modifications associated with supersonic transport flights in the stratosphere and other products of man's activities.

ACKNOWLEDGEMENTS

The authors wish to thank the Environment Rocket Sounding System, managed by the 6th Weather Wing, Andrews Air Force Base, Md. for materiel support and the Geophysics Division, Pacific Missile Range, Point Mugu, Calif. for logistic and operational support in the rocket flights noted above. We are also grateful to R. Auluck and P. C. Swartz for assistance in the BUV and rocket data processing and R. D. Westcott for digital conversion of the rocket data.

REFERENCES

Anderson, G. P., C. A. Barth, F. Cayla, and J. London, Satellite observations of the vertical ozone distribution in the upper stratosphere, Annales de Geophysique, 25, (1969), 341-345.

Barnett, J. J., M. J. Cross, R. S. Harwood, J. T. Houghton, C. G. Morgan, G. E. Peckham, C. D. Rodgers, S. D. Smith, and E. J. Williamson. The first year of the selective chopper radiometer on Nimbus 4, Quart. J. R. Met. Soc., 98, (1972), 17-37.

Dütsch, H. U., Vertical ozone distribution from Umkehr observations, Arch. Meteorol. Geophys. Biok. A, 11, (1959), 240-251.

Green, A. E. S., Attenuation by ozone and the earth's albedo in the middle ultraviolet, Appl. Opt., 3, (1964), 203-208.

Heath, D. F., A. J. Krueger, and C. L. Mateer, The Nimbus 4 Backscatter Ultraviolet (BUV) atmospheric ozone experiment — two years operation, PAGEOPH, to be published.

Herman, B. M., and D. N. Yarger, Estimating the vertical atmospheric ozone distribution by inverting the radiative transfer equation for pure molecular scattering, J. Atmos. Sci., 26, (1969), 153-162.

Hilsenrath, E., L. Seiden, and P. Goodman: An ozone measurement in the mesosphere and stratosphere by means of a rocket sonde. J. Geophys. Res., 74, (1969), 6873-6879.

Iozenas, V. A., Determining the vertical ozone distribution in the upper atmospheric layers from satellite measurements of ultraviolet solar radiation scattered by the earth's atmosphere, Geomag. Aeron., 8, (1968), 403-407.

Iozenas, V. A., V. A. Krasnopol'skiy, A. P. Kuznetsov, and A. J. Lebedinsky, Studies of the earth's ozonosphere from satellites, Izv. Atmos. Oceanic Phys., 5, (1969a), 77-82.

Iozenas, V. A., V. A. Krasnopol'skiy, A. P. Kuznetsov, and A. J. Lebedinsky, An investigation of the planetary ozone distribution from satellite measurements of ultraviolet spectra, Izv. Atmos. Oceanic Phys., 5, (1969b), 219-233.

Krasnopol'skiy, V. A., The ultraviolet spectrum of solar radiation reflected by the terrestrial atmosphere and its use in determining the total content and vertical distribution of atmospheric ozone, Geomag. Aeron., 6, (1966), 236-242.

Krueger, A. J., Rocket measurements of ozone over Hawaii, Ann Geophys., 25, (1969), 307-311.

Mateer, C. L., On the information content of Umkehr observations, J. Atmos. Sci., 22, (1965), 370-381.

Mateer, C. L., A review of some aspects of inferring the ozone profile by inversions of ultraviolet radiance measurement, in The Mathematics of Profile Inversion, (ed. by L. Colin), NASA TMX-62150, (1972), 2-25.

Nimbus Project, The Nimbus 4 User's Guide, National Space Science Data Center, Goddard Space Flight Center, Greenbelt, Maryland, (1970).

Rawcliffe, R. D., and D. D. Elliott, Latitude distributions of ozone at high altitudes, deduced from satellite measurement of the earth's radiance at 2840A, J. Geophys. Res., 71, (1966), 5077-5089.

Singer, S. F., and R. C. Wentworth, A method for the determination of the vertical ozone distribution from a satellite, J. Geophys. Res., 62, (1957), 299-308.

Smith, W. L., Iterative solution of the radiative transfer equation for the temperature and absorbing gas profile of an atmosphere, Appl. Opt., 9, (1970), 1993-1999.

Strand, O. N., Theory and methods related to the singular-function expansion and Landweber's iteration for solving integral equations of the first kind, SIAM J. Num. Anal., in Press, 1972.

Twomey, S., On the numerical solution of Fredholm integral equations of the first kind by the inversion of the linear system produced by quadrature, J. Assoc. Comp. Mach., 10, (1963), 97-101.

Yarger, D. N., An evaluation of some methods of estimating the vertical atmospheric ozone distribution from the inversion of spectral ultraviolet radiation, J. Appl. Meteor., 9, (1970), 921-928.